

## CHAPTER 3

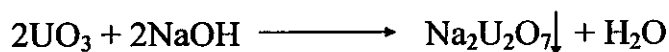
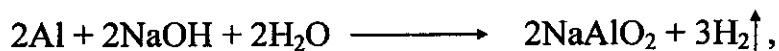
### RESULTS AND DISCUSSION

#### 3.1. Preparation of the fission-product feeding solutions:

Fission-product (FP) solutions were prepared from  $4 \times 0.025$  g  $\text{UO}_3$  targets wrapped in thin aluminum foils and irradiated in the ETRR-2 Research Reactor for 4 h at a thermal neutron flux of  $1 \times 10^{14}$   $\text{n.cm}^{-2}.\text{s}^{-1}$ . Thereafter, they were either cooled for 10 d (i.e., hot targets) or decayed for  $\sim 2.5$  y (i.e., aged targets) before chemical processing as in the sequence mentioned below.

##### 3.1.1. Sodium hydroxide digestion:

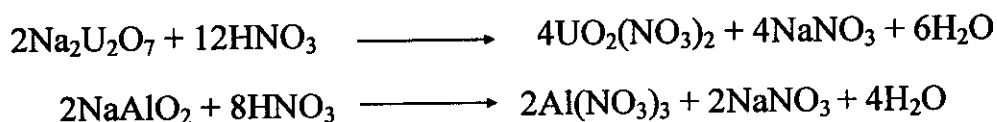
The irradiated  $\text{UO}_3$  targets with their aluminum containing foils were initially digested in 10 ml 2 M NaOH solution for  $\sim 24$  h in the digestion system (Figure 2.1). The digestion process resulted in dissolution of the aluminum foils forming sodium aluminate (Foster et al., 1955; Agasyan, 1980; Pajunen, 1999) and the formation of sodium diuranate which remains as undissolved residue (Cordfunke, 1969; Etherington, 1958) according to the following equations:



##### 3.1.2. Nitric acid treatment:

The three-neck bottle containing the mixture of the soluble FP supernatant and the diuranate residue together with the insoluble and partially soluble FP's was connected to the distillation system (Figure 2.2). The mixture was acidified with concentrated  $\text{HNO}_3$  acid to obtain a completely soluble FP solution in 20 %  $\text{HNO}_3$ . In the acidification step, diuranate dissolves giving uranyl nitrate (Bonini

et al., 1998), while sodium aluminate gives aluminum nitrate (Agasyan, 1980) according to:



### 3.1.3. Advantages of the alkali/acid dissolution process:

Immediate acid dissolution of the irradiated uranium targets requires addition of  $\text{Hg}^{2+}$  ion, e.g.,  $\text{Hg}(\text{NO}_3)_2$ , as a catalyst to dissolve the aluminum foils, which generates a mixed-waste stream of both radionuclides and mercury components. The generation of mixed waste is undesirable with respect to waste minimization, cost of treatment and discarding (William et al., 2000). The presence of mercury is also undesirable in chemical processing, because of its possible chemical interfering and toxicity (Roesmer, 1970).

The coupled alkali digestion/acid dissolution processes compiles the advantages of both the separate procedures and avoids their sequence disadvantages (Vandegrift et al., 1997). Like in the alkali digestion, fission-produced noble-gases, such as krypton and xenon, are released and can be recovered separately from radioiodine which, mainly, remains in the fission-product solution. Like in acid dissolution, the total fission-produced radionuclides (except noble-gasses and acid-volatile species) are completely contained in the prepared FP solution, after the acidification step, which is advantageous in maximization of the recovery yields of alkali insoluble and/or partially soluble radionuclides, e.g.,  $^{103,106}\text{Ru}$  and  $^{95}\text{Zr}/^{95}\text{Nb}$  (El-Absy, 1991; Eid, 1999; Mostafa 2002).

### 3.2. Gamma-ray spectrometric analysis of FP feeding solutions:

#### 3.2.1. Hot FP feeding solution:

Figure 3.1 shows gamma-ray spectra of the supernatant obtained from digestion of the hot  $\text{UO}_3$  targets in 2 M NaOH solution (a), the formed residue (b), and the FP solution in 20 %  $\text{HNO}_3$  acid. According to the gamma-ray energy peaks appeared in Figure 3.1, the radionuclides of  $^{99}\text{Mo}$  ( $T_{1/2} = 2.75$  d,  $Y_f = 6.11$  %) /  $^{99\text{m}}\text{Tc}$  ( $T_{1/2} = 6.01$  h,  $Y_f = 5.38$  %),  $^{136}\text{Cs}$  ( $T_{1/2} = 13.16$  d,  $Y_f = 5.47 \times 10^{-3}$  %), and  $^{137}\text{Cs}$  ( $T_{1/2} = 30.07$  y,  $Y_f = 6.19$  %) /  $^{137\text{m}}\text{Ba}$  ( $T_{1/2} = 2.55$  min,  $Y_f = 5.85$  %) were completely included in the alkali supernatant (a), while the radionuclides of  $^{140}\text{Ba}$  ( $T_{1/2} = 12.75$  d,  $Y_f = 6.21$  %),  $^{140}\text{La}$  ( $T_{1/2} = 1.68$  d,  $Y_f = 6.22$  %),  $^{141}\text{Ce}$  ( $T_{1/2} = 32.5$  d,  $Y_f = 5.85$  %),  $^{144}\text{Ce}$  ( $T_{1/2} = 284.6$  d,  $Y_f = 5.5$  %),  $^{147}\text{Nd}$  ( $T_{1/2} = 10.98$  d,  $Y_f = 2.25$  %),  $^{155}\text{Eu}$  ( $T_{1/2} = 4.71$  y,  $Y_f = 3.21 \times 10^{-2}$  %) and  $^{239}\text{Np}$  ( $T_{1/2} = 2.36$  d, neutron-activation radionuclide) were completely included in the residue (b). The radionuclides of  $^{95}\text{Zr}$  ( $T_{1/2} = 64.02$  d,  $Y_f = 6.5$  %),  $^{95}\text{Nb}$  ( $T_{1/2} = 34.97$  d,  $Y_f = 6.5$  %),  $^{103}\text{Ru}$  ( $T_{1/2} = 39.27$  d,  $Y_f = 3.03$  %),  $^{131}\text{I}$  ( $T_{1/2} = 8.04$  d,  $Y_f = 2.89$  %),  $^{132}\text{I}$  ( $T_{1/2} = 2.28$  h,  $Y_f = 4.31$  %), and  $^{132}\text{Te}$  ( $T_{1/2} = 3.26$  d,  $Y_f = 4.3$  %) were distributed between the supernatant (a) and the residue (b) with different ratios, and all of the radionuclides in (a) and (b) were completely included in the acidic solution obtained by acidifying the mixture of the alkali supernatant and the residue with  $\text{HNO}_3$  acid (c). In the present work, the given decay-energies were cited from Burrows (1988), Baglin and Chu (1998), and Chu et al. (1999), whereas fission-yields and half-lives were cited from Etherington (1958) and England and Rider (1993).

Some of the long-lived radioisotopes could not be detected in the gamma-ray spectra of the hot FP solution but they were detected in those of the aged FP solution as mentioned below.

Counts per channel, arbitrary units

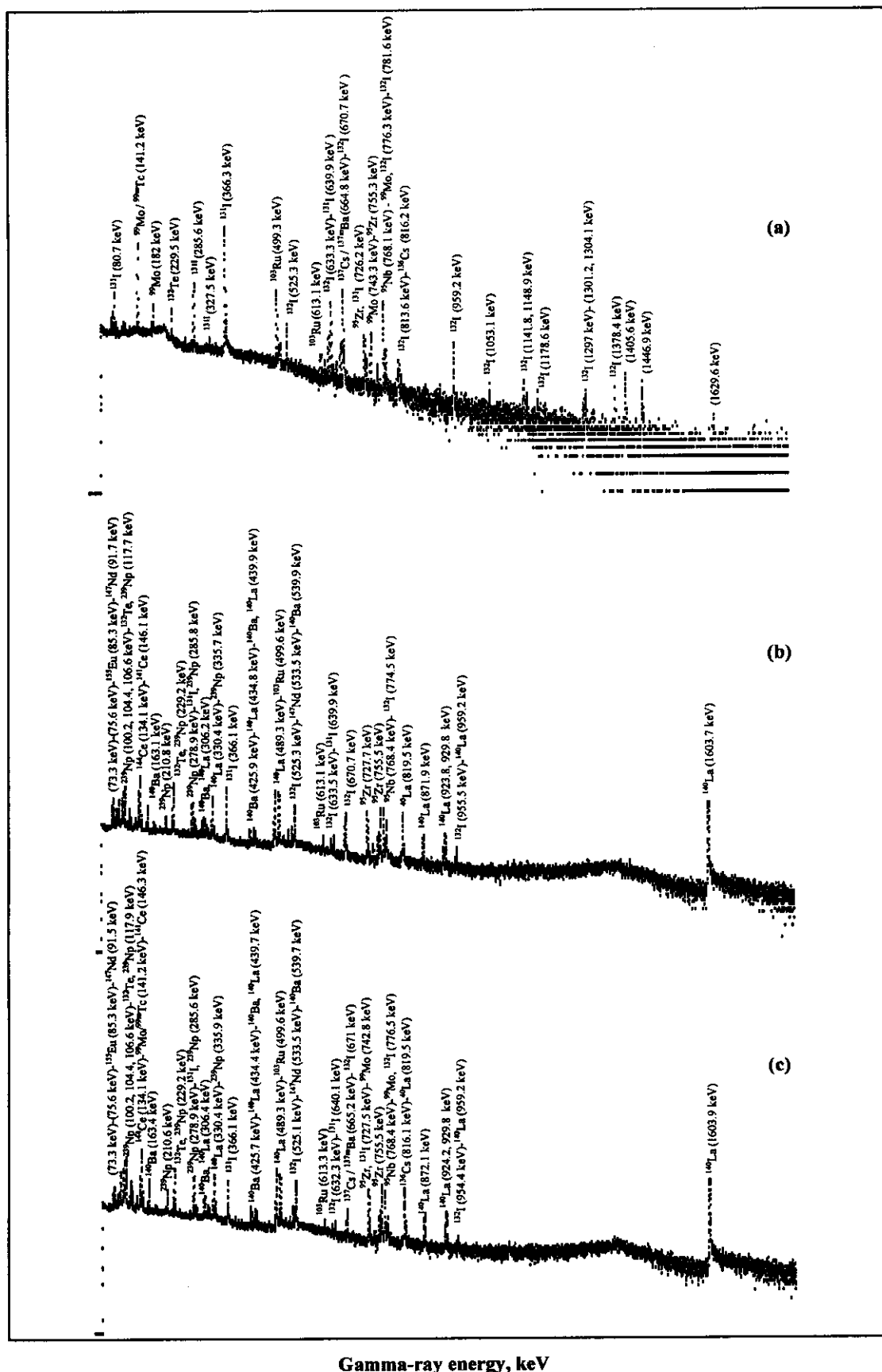


**Figure 3.1.** Gamma-ray spectra of the supernatant (a) and residue (b) of the hot  $\text{UO}_3$  targets (obtained from  $4 \times 0.025$  g  $\text{UO}_3$  targets irradiated in ETRR-2 Reactor for 4 h at a thermal neutron flux of  $1 \times 10^{14}$  n.cm $^{-2}$ .s $^{-1}$  and cooled for 10 d) digested in 10 ml 2 M NaOH solution for ~ 24 h and of the FP solution in 20 %  $\text{HNO}_3$  (c).

### 3.2.2. Aged FP feeding solution:

Figure 3.2 shows gamma-ray spectrum of the aged FP solution in 20 %  $\text{HNO}_3$  acid. The detected gamma-ray energy peaks were those characteristic for the long-lived fission-produced radionuclides of  $^{106}\text{Ru}$  ( $T_{1/2} = 1.02$  y,  $Y_f = 0.402$  %) /  $^{106}\text{Rh}$  ( $T_{1/2} = 29.9$  s,  $Y_f = 0.402$  %),  $^{125}\text{Sb}$  ( $T_{1/2} = 2.76$  y,  $Y_f = 0.034$  %),  $^{137}\text{Cs}$  ( $T_{1/2} = 30.07$  y,  $Y_f = 6.19$  %) /  $^{137\text{m}}\text{Ba}$  ( $T_{1/2} = 2.552$  min,  $Y_f = 5.85$  %),  $^{144}\text{Ce}$  ( $T_{1/2} = 284.6$  d,  $Y_f = 5.5$  %) /  $^{144}\text{Pr}$  ( $T_{1/2} = 17.28$  m,  $Y_f = 5.5$  %), and  $^{155}\text{Eu}$  ( $T_{1/2} = 4.71$  y,  $Y_f = 3.21 \times 10^{-2}$  %) along with the neutron-activation radionuclides of  $^{60}\text{Co}$  ( $T_{1/2} = 5.27$  y),  $^{65}\text{Zn}$  ( $T_{1/2} = 243.8$  d), and  $^{134}\text{Cs}$  ( $T_{1/2} = 2.065$  y) originated from stable chemical impurities of the target material and/or of its aluminum wrapper (Lin, 1996; Carlton et al., 1999; PNNL, 2003). Again, some of the long-lived fission-produced radionuclides were not detected in the obtained gamma-ray spectrum in Figure 3.2 because of their low fission-yields, e.g.,  $^{146}\text{Pm}$  ( $T_{1/2} = 5.53$  y,  $Y_f = 4.5 \times 10^{-10}$  %), low gamma-ray abundance, e.g.,  $^{99}\text{Tc}$  ( $T_{1/2} = 2.1 \times 10^5$  y,  $E_\gamma = 89.65$  keV,  $6 \times 10^{-4}$  %) and  $^{90}\text{Sr}$  ( $T_{1/2} = 29.1$  y,  $E_\gamma = 1743$  and  $1758$  keV,  $1.02 \times 10^{-2}$  and  $1.26 \times 10^{-3}$  %, respectively, from its daughter  $^{90}\text{Y}$ ), low-energy, e.g.,  $^{151}\text{Sm}$  ( $T_{1/2} = 90$  y;  $E_\gamma = 21.54$  keV), absence of gamma-ray emission, e.g.,  $^{135}\text{Cs}$  ( $T_{1/2} = 2.3 \times 10^6$  y), and/or interference between gamma-ray photopeaks of converging values. Generally, this interference decreases with the progression of the chemical separation processes leading to the appearance of some overlapped and/or highly diluted radionuclides. For instance, the neutron-activation product  $^{152}\text{Eu}$  ( $T_{1/2} = 13.48$  y) was detected in the gamma-ray spectra obtained after separation of the bulk of the  $^{137}\text{Cs}/^{137\text{m}}\text{Ba}$  couple. Strontium-90 radionuclide could be detected and identified when it was concentrated onto an ion-exchange matrix as mentioned below.

Table 3.1 gives comparison of radioisotopes detected in the gamma-ray spectra of hot and aged FP solutions in 20 %  $\text{HNO}_3$  acid.

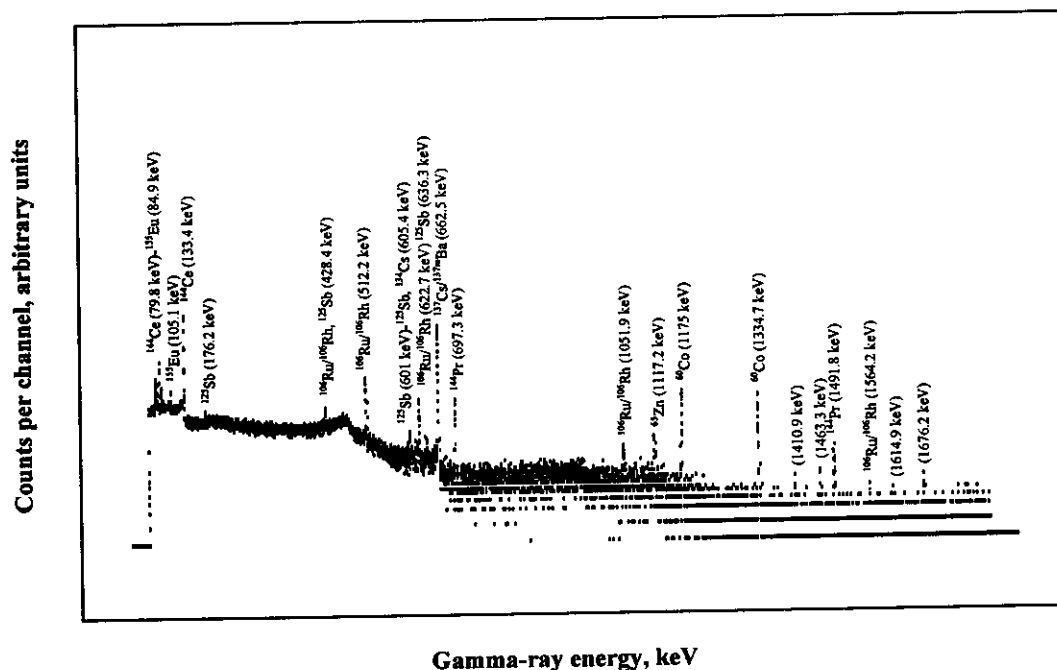


**Figure 3.2.** Gamma-ray spectrum of the aged FP solution in 20 %  $\text{HNO}_3$  acid (obtained by digestion of  $4 \times 0.025$  g  $\text{UO}_3$  targets, irradiated in ETRR-2 Reactor for 4 h at a thermal neutron flux of  $1 \times 10^{14} \text{ n.cm}^{-2}.\text{s}^{-1}$  and aged for  $\sim 2.5$  y, in 10 ml of 2 M NaOH for  $\sim 24$  h and addition of concentrated  $\text{HNO}_3$  acid to dissolve the formed residue).

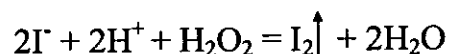
**Table 3.1.** Comparison of radioisotopes detected in the gamma-ray spectra of the hot and aged FP solutions.

Hot FP feeding solution			Aged FP feeding solution		
Radioisotope	Half-life, $T_{1/2}$	Fission yield, $Y_f$	Radioisotope	Half-life, $T_{1/2}$	Fission yield, $Y_f$
$^{103}\text{Ru}$	39.27 d	3.03 %	$^{106}\text{Ru}$ $\downarrow \beta^-$ $^{106}\text{Rh}$	1.02 y	0.402 %
				29.9 s	0.402 %
$^{137}\text{Cs}$ $\downarrow \beta^-$ $^{137\text{m}}\text{Ba}$	30.07 y	6.19 %	$^{137}\text{Cs}$ $\downarrow \beta^-$ $^{137\text{m}}\text{Ba}$	30.07 y	6.19 %
	2.55 min	5.85 %		2.55 min	5.85 %
$^{141}\text{Ce}$	32.5 d	5.85 %	$^{144}\text{Ce}$ $\downarrow \beta^-$ $^{144}\text{Pr}$	284.6 d	5.5 %
$^{144}\text{Ce}$	284.6 d	5.5 %		17.28 min	5.5 %
$^{155}\text{Eu}$	4.71 y	$3.21 \times 10^{-2}$ %	$^{155}\text{Eu}$	4.71 y	$3.21 \times 10^{-2}$ %
$^{95}\text{Zr}$ $\downarrow \beta^-$ $^{95}\text{Nb}$	64.02 d	6.5 %	$^{125}\text{Sb}$	2.76 y	0.034 %
	34.97 d	6.5 %	$^{60}\text{Co}$	5.27 y	Neutron-activation radionuclide
$^{99}\text{Mo}$ $\downarrow \beta^-$ $^{99\text{m}}\text{Tc}$	2.75 d	6.11 %	$^{65}\text{Zn}$	243.8 d	Neutron-activation radionuclide
	6.01 h	5.38 %			
$^{131}\text{I}$	8.04 d	2.89 %			
$^{132}\text{Te}$ $\downarrow \beta^-$ $^{132}\text{I}$	3.26 d	4.3 %			
	2.28 h	4.31 %			
$^{136}\text{Cs}$	13.16 d	$5.47 \times 10^{-3}$ %			
$^{140}\text{Ba}$ $\downarrow \beta^-$ $^{140}\text{La}$	12.75 d	6.21 %			
	1.68 d	6.22 %			
$^{147}\text{Nd}$	10.98 d	2.25 %			
$^{239}\text{Np}$	2.36 d	Neutron-activation radionuclide			

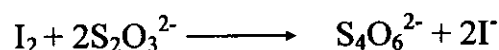
### 3.3. Separation of radioiodine:

To the FP solution in 20 % HNO<sub>3</sub> acid, contained in the three-neck bottle of the distillation system (Figure 2.2), 0.5 ml of 30 % H<sub>2</sub>O<sub>2</sub> was added. Then, it was boiled till free from iodine radionuclides. An air current was passed through the FP solution during the distillation process to carry out the distilled off radioiodine. In case of the hot FP solution, the air current carrying <sup>131,132</sup>I was passed through an acid trap containing 15 ml 3 M H<sub>2</sub>SO<sub>4</sub>, two ice-cooled alkali receivers containing 15 and 5 ml 0.1 M NaOH-0.01 M Na<sub>2</sub>S<sub>2</sub>O<sub>3</sub>, respectively, and finally in a liquid nitrogen-cooled AgNO<sub>3</sub>-impregnated charcoal filter. For the aged FP solution, the distilled off <sup>129</sup>I passed through the same installation arrangements without the acid trap.

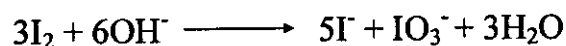
In acid solutions and in the presence of H<sub>2</sub>O<sub>2</sub>, iodide ions are converted to molecular iodine according to the following equation (Kahn and Kleinberg, 1977; Vogel, 1961):



The distilled off radioiodine was recovered in the NaOH solution containing Na<sub>2</sub>S<sub>2</sub>O<sub>3</sub> to verify its existence as I<sup>-</sup> ion according to the following equation (IAEA, 1971; Agasyan, 1980):



Also, the presence of S<sub>2</sub>O<sub>3</sub><sup>2-</sup> protects the recovered radioiodine against radiolytic oxidation, since the absence of such reducing anion leads to the formation of the iodate ion, IO<sub>3</sub><sup>-</sup>, along with I<sup>-</sup> in the ratio of 1:5, respectively, according to the following equation (Abdukayumov et al., 2000):





### 3.3.1. Separation of $^{131}\text{I}$ from the hot FP solution:

#### 3.3.1.1. Separation yield of $^{131}\text{I}$ :

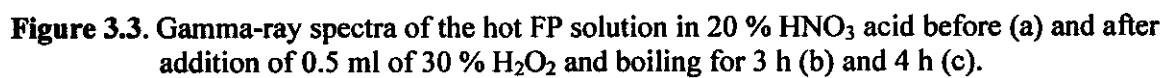
Figure 3.3 (a, b, and c) shows gamma-ray spectra of the hot FP solution in 20 %  $\text{HNO}_3$  containing  $\text{H}_2\text{O}_2$  before boiling and after boiling for 3 h and 4 h, respectively. As indicated by the radiometric assay data, it was found that boiling for 4 h was sufficient for separation of  $\geq 99.99$  % of  $^{131}\text{I}$  from the hot FP solution. The obtained data were in agreement with our previously obtained results for separation of  $^{131}\text{I}$  from FP solution in 20 %  $\text{H}_2\text{SO}_4$  acid containing  $\text{H}_2\text{O}_2$  as an oxidant (El-Absy et al., 2004)

#### 3.3.1.2. Recovery yield of $^{131}\text{I}$ :

Radiometric assay data indicated that 15.4 % of the distilled off  $^{131}\text{I}$  was retained in the acid trap, whereas 82.7 % of it was collected in the first alkali receiver and no measurable radioactivity was detected in the second alkali receiver. The remaining ratio, 1.9 % of  $^{131}\text{I}$ , might be deposited on the glass walls of the distillation system. The fraction of radioiodine retained in the acid trap might be due to the formation of oxygenated species of iodine along with  $\text{I}_2$  during the distillation process. For example,  $\text{HIO}_3$  gives  $\text{IO}_2\text{HSO}_4$  in a dilute solution of sulfuric acid. Also iodosyl sulfate,  $(\text{IO})_2\text{SO}_4$ , can be obtained by the action of  $\text{H}_2\text{SO}_4$  on  $\text{I}_2\text{O}_5$  (Cotton and Wilkinson, 1979). The retention of such species in the acid trap before recovery of the distilled  $^{131}\text{I}$  in the alkali solution was necessary to enhance the radiochemical purity of  $^{131}\text{I}$  as  $\text{I}^-$  ion.

#### 3.3.1.3. Radionuclidic purity of $^{131}\text{I}$ :

Figure 3.4 (a, b, and c) shows gamma-ray spectra of the acid trap (measured immediately at the end of the distillation process) and the first alkali receiver containing 0.1 M  $\text{NaOH}$ -0.01 M  $\text{Na}_2\text{S}_2\text{O}_3$  measured immediately at the end of the distillation process and after  $\sim 40$ -h decay time, respectively. As shown in Figure 3.4 (a and b), no other radionuclides existed along with  $^{131}\text{I}$  and



Counts per channel, arbitrary units

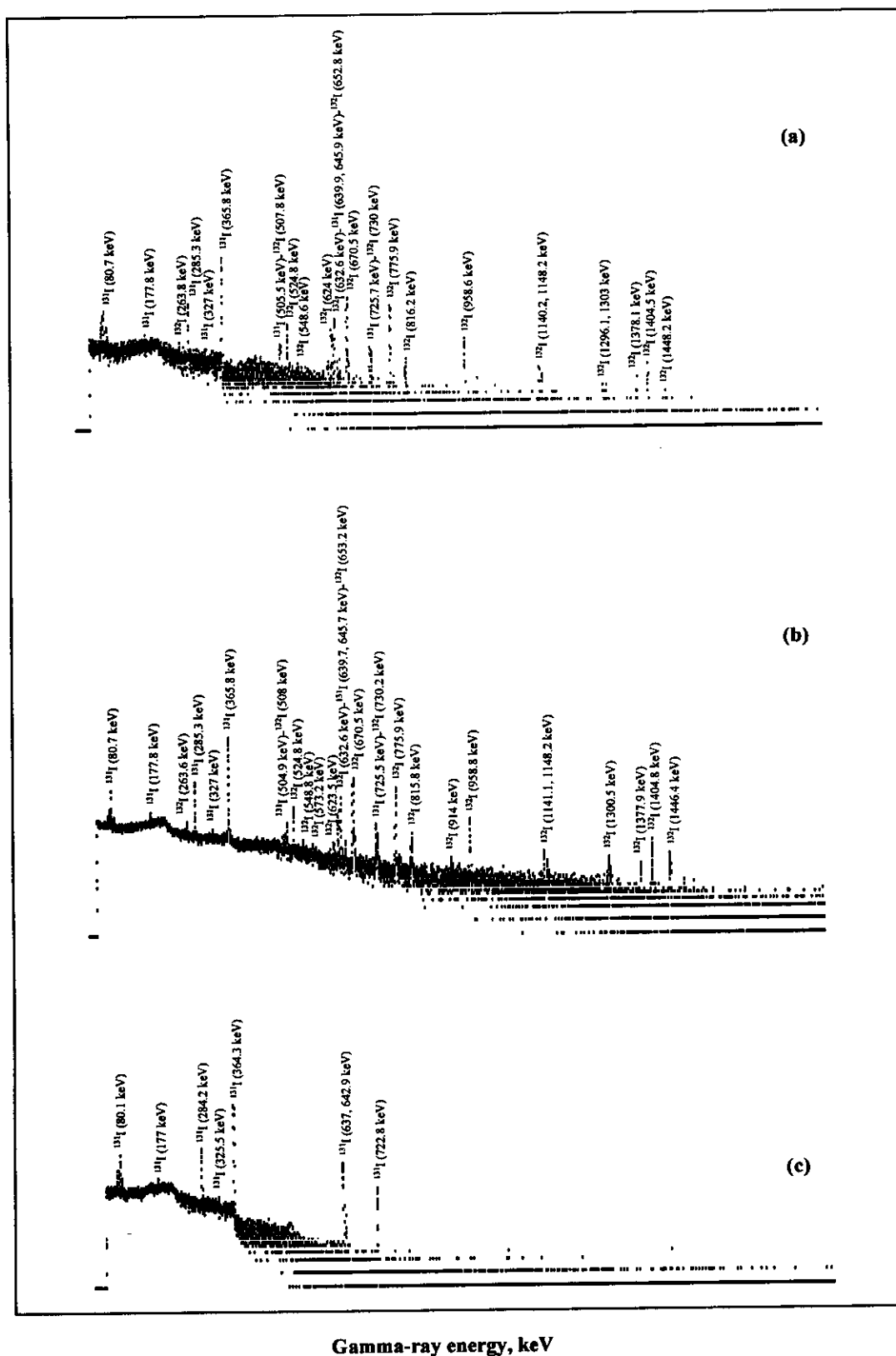


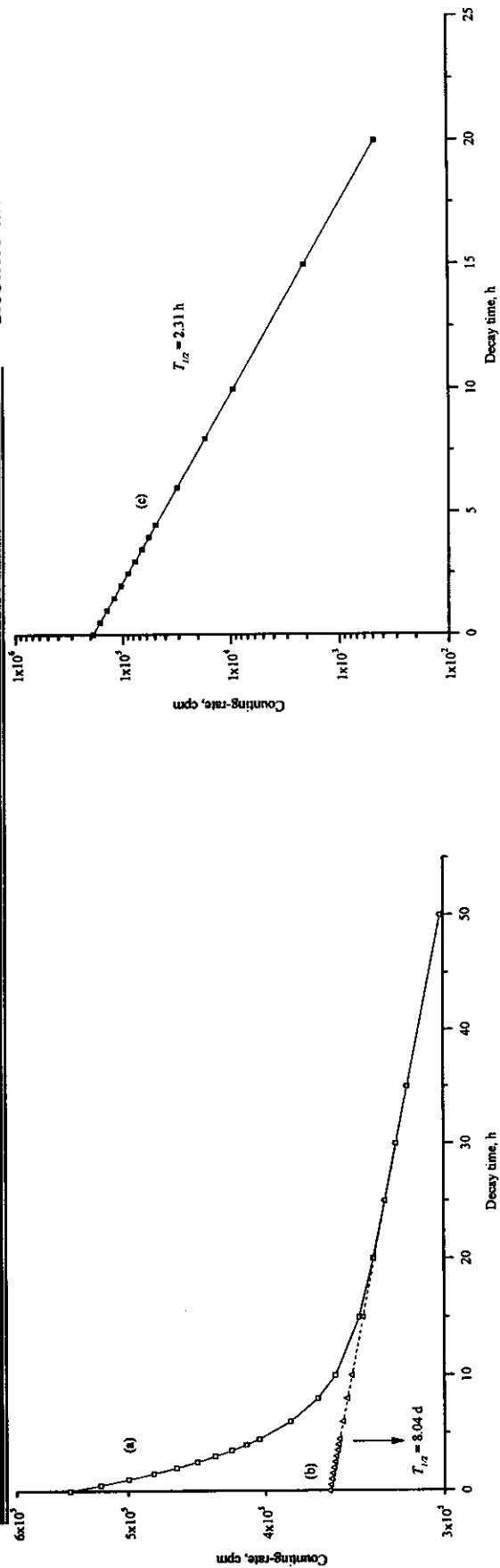
**Figure 3.4.** Gamma-ray spectra of the acid trap (3 M  $\text{H}_2\text{SO}_4$ ) measured immediately at the end of the distillation process (a) and the first alkali receiver (0.1 M  $\text{NaOH}$ -0.01M  $\text{Na}_2\text{S}_2\text{O}_3$ ) measured at the end of the distillation process immediately (b) and after ~ 40-h decay time (c).

$^{132}\text{I}$  in both of the acid trap and the first alkali receiver. No iodine or any other radioisotopes were detected neither in the second alkali receiver nor in the charcoal filter. Radiometric assay data indicated that radionuclidic purity of the recovered  $^{131}\text{I}$ , at the end of the distillation process, was found to be 65.60 % with the presence of 34.40 %  $^{132}\text{I}$  ( $T_{1/2} = 2.28$  h) as the only detected radiocontaminant in the alkali receiver solution. Iodine-132 radionuclide generated from nuclear decay of  $^{132}\text{Te}$  ( $T_{1/2} = 3.26$  d) existed in the hot FP solution. However, radionuclidic purity of the recovered  $^{131}\text{I}$  enhanced gradually to reach  $\geq 99.99$  %  $^{131}\text{I}$  after complete decay of  $^{132}\text{I}$ , i.e., after  $\sim 40$  h as shown in Figure 3.4 (c). After 5 months have been elapsed, no residual radioactivity was detected in the first alkali receiver containing the radioiodine product.

The radionuclides found in the  $^{131}\text{I}$  product collected in the first alkali receiver ( $^{131}\text{I}$  and  $^{132}\text{I}$ ) were further identified by their characteristic half-lives obtained from their decay curves as shown in Figure 3.5 (a, b, c, and d). As indicated by Figure 3.5 (c and d), two straight lines were obtained their slopes are corresponding to the half-lives of  $^{132}\text{I}$  and  $^{131}\text{I}$  radionuclides, respectively.

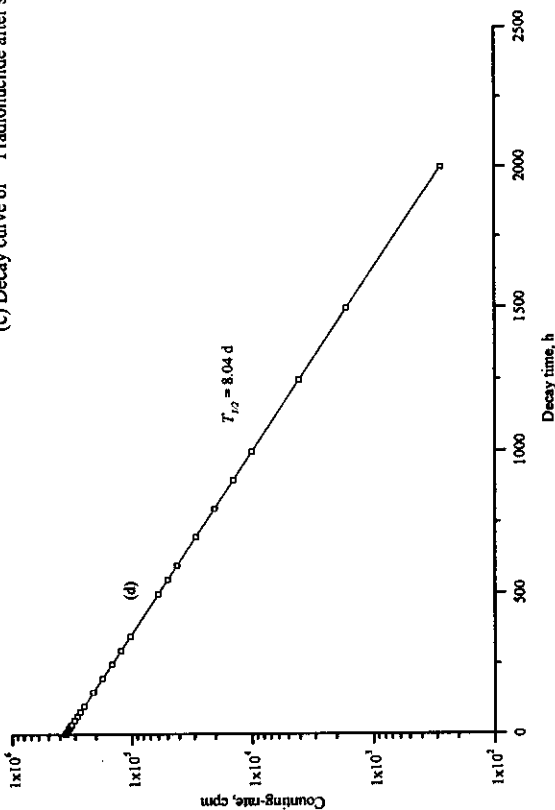
#### 3.3.1.4. Radiochemical purity of $^{131}\text{I}$ :

Radiochemical purity of the  $^{131}\text{I}$ -product solution was determined by the ascending paper chromatography method using a strip of "Whatman No. 1" paper (30 cm long and 5 cm wide), as a stationary phase, and a mixture of 70 % methanol and 30 %  $\text{H}_2\text{O}$ , as the developing mobile phase. In this method, one  $R_f$  value of 0.73 was obtained in agreement with the published  $R_f$  value (0.7). This value refers to the presence of  $\text{I}^-$  and/or  $\text{I}_3^-$  ions (Baldwin, 1986). Alternatively, the same procedure was carried out using a strip of silica gel TLC (30 cm long and 5 cm wide) and a solvent of a mixture of isopropyl alcohol, ethyl acetate, 6 M ammonium hydroxide, and acetone (35:30:25:20 by volume, respectively). In



(a and b) Decay curves of the gross radioactivity of the iodine-product solution (a) and extrapolation of the decay curve tail (b).

(c) Decay curve of  $^{132}\text{I}$  radionuclide after subtraction of the radioactivity of the long-lived  $^{131}\text{I}$  radionuclide (curve b).



(d) Decay curve of  $^{131}\text{I}$  radionuclide after subtraction of the radioactivity of the short-lived  $^{132}\text{I}$  radionuclide (curve a).

Figure 3.5. Decay curves of the radioiodine recovered from the hot FP solution in the alkali receiver (0.1 M NaOH-0.01 M  $\text{Na}_2\text{S}_2\text{O}_3$ ).

this case,  $R_f$  value of 0.8 was obtained in agreement with the published  $R_f$  value (0.82) which refers to the presence of  $I^-$  ion (Baldwin, 1986). Figure 3.6 (a and b) shows the radiochromatograms of the  $^{131}I$ -product solution obtained by using “Whatman No.1” chromatographic paper and silica gel TLC, respectively. Radiochemical purity with “Whatman No.1” chromatographic paper and with silica gel TLC was found to be 99.4 % and 99.2 % as  $I^-$ , respectively. These values are suitable for use of  $^{131}I$  product in medical applications (Isselt et al., 2000). It is worth mentioning that thyroid only fixes iodine in the form of iodide ions (Čvorić, 1969).

#### **3.3.1.5. pH-value of the $^{131}I$ -product solution:**

At the end of the distillation process, pH-value of the first alkali receiver containing the recovered  $^{131}I$  was found to be 12.8. This pH-value is suitable to avoid formation of volatile elemental iodine. Generally, the rate of formation of  $I_2$  by radiolytic oxidation of  $I^-$  appears to fall with increasing the pH-value at least over the range of pH 4-9. The higher the pH-value, the higher the ratio of iodine remains in the  $I^-$  form. The minimum or optimum pH-value is uncertain but the rate of  $I_2$  formation only falls by a factor of 1.3 between pH 6 and pH 7 but a further higher factor of 2.6 between pH 7 and pH 8 was reported (Ashmore et al., 1996).

#### **3.3.1.6. Radioactivity and radioactive concentration of the $^{131}I$ -product solution:**

Radioactivity of the recovered  $^{131}I$ ,  $A_{I-131}$ , was calculated according to the following equation:

$$A_{I-131} = R_{I-131} ( A_{0(I-131)} e^{-\lambda_{I-131} t_{e(I-131)}} ) \quad (3.1)$$

Where,

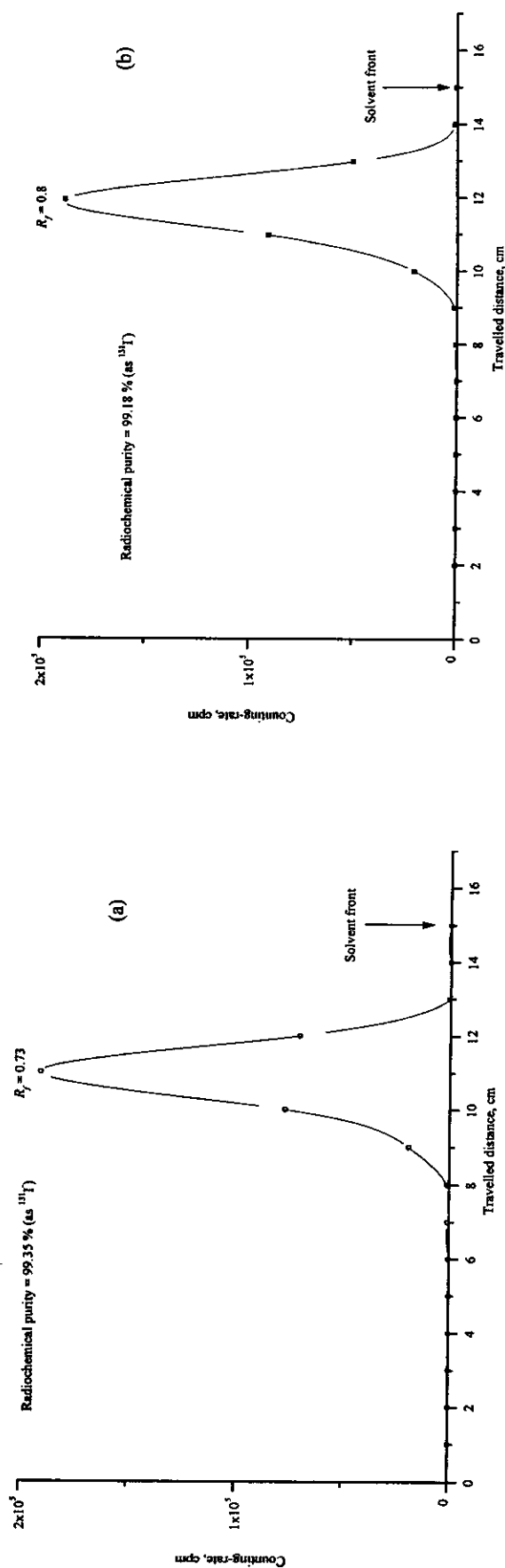


**Figure 3.6.** Radiochromatograms of the  $^{131}\text{I}$  product solution obtained by ascending paper chromatography method using a strip of "Whatman No. 1" chromatographic paper (30 cm long and 5 cm wide) and a mixture of 70 % methanol and 30 %  $\text{H}_2\text{O}$  as a developing solvent (a) and a strip of TLC with silica gel (30 cm long and 5 cm wide) and a mixture of isopropyl alcohol, ethyl acetate, 6 M ammonium hydroxide, and acetone (35:30:25:20 by volume, respectively) as a developing solvent.

$A_{0(I-131)}$  = radioactivity of  $^{131}\text{I}$  initially present at the end of irradiation,  
calculated by using Equation 1.3 (37 MBq).

$R_{I-131}$  = recovery yield of  $^{131}\text{I}$  (82.7 %).

$\lambda_{I-131}$  = decay constant of  $^{131}\text{I}$  ( $3.59 \times 10^{-3} \text{ h}^{-1}$ ).

$t_{e(I-131)}$  = elapsed time period from the end of irradiation to completion of  $^{131}\text{I}$   
separation (269 h; cooling time = 240 h and processing time = 29 h).

Radioactive concentration of the recovered  $^{131}\text{I}$ ,  $C_{I-131}$ , was calculated according  
to the equation:

$$C_{I-131} = A_{I-131} / V_{I-131} \quad (3.2)$$

Where,

$V_{I-131}$  = volume of the  $^{131}\text{I}$ -product solution (15 ml).

According to Equations 3.1 and 3.2, radioactivity and radioactive concentration  
of the recovered  $^{131}\text{I}$  were found to be 11.7 MBq and 0.8 MBq/ml, respectively.  
Table 3.2 compiles the specifications and quality control data of the  $^{131}\text{I}$  product.

### 3.3.2. Separation of $^{129}\text{I}$ from the aged FP solution:

The aged FP solution in 20 %  $\text{HNO}_3$  containing  $\text{H}_2\text{O}_2$  was boiled for 4 h  
to distill the long-lived  $^{129}\text{I}$  radionuclide. Under similar conditions, the boiling  
time was sufficient to distill  $^{131}\text{I}$  from the hot FP solution (Section 3.3.1). Iodine-  
129 radionuclide ( $T_{1/2} = 1.57 \times 10^7 \text{ y}$ ,  $Y_f = 3.38 \%$ ) was not detected in the  
obtained gamma-ray spectra of the alkali receivers as well as in the FP solutions  
obtained before and after boiling for 4 h. This may be due to decay of  $^{129}\text{I}$  to  
stable  $^{129}\text{Xe}$  with emission of characteristic gamma-rays of low-energy (29.78  
keV). Also, no gamma-ray photopeaks of interfering radionuclides were  
detected in the obtained gamma-ray spectra of the alkali receiver, which verify  
the above mentioned data for separation and radionuclidic purity of  $^{131}\text{I}$ .